

# Colloidal Quantum Dots-Based Upconversion Devices

Subjects: [Quantum Science & Technology](#)

Contributor: Xin Tang , Tianyu Rao , Menglu Chen , Ge Mu

Colloidal quantum dots (CQD) have narrow emission linewidth and adjustable bandgap, so that CQD based infrared detectors can realize a widely tunable infrared spectral range. In addition, the luminescence spectrum of CQDs is extremely narrow, the color saturation and purity are high, and the optical stability is excellent, which can be obtained by solution procession. Therefore, CQDs-based LEDs (QLEDs) have excellent performances of a wide color gamut, long life, and low cost. For CQD baesd upconverters, except for the top electrode, the entire device can be prepared by solution method, which greatly simplifies the preparation of the device and make the upconverters are available for use in the fields of flexible devices.

infrared-to-visible upconversion devices

infrared imaging

colloidal quantum dots

## 1. NIR-to-Visible Upconversion

In 2011, Kim and his co-workers reported their achievement of a low-cost upconversion device with infrared sensitivity up to 1.5  $\mu\text{m}$  using PbSe inorganic colloidal nanocrystals as infrared PD. It was the first time that the NIR-to-visible light converter of CQDs' integrated phosphorescent emitting OLED was reported, the structure and schematic diagram are shown in **Figure 1a,b**. It must be known that all-organic upconversion devices before this work nearly had no infrared sensitivity beyond 1  $\mu\text{m}$ , moreover, there were not any hybrid devices that could reach a 1.3% photon-to-photon conversion efficiency (that this work obtained) in the past. In contrast to previous studies, Kim et al. employed a wide bandgap ZnO layer as a hole blocking layer to improve the on/off ratio of the device, and the dark current of the device was obviously reduced, moreover the signal-to-noise ratio of the device was increased [\[1\]](#).

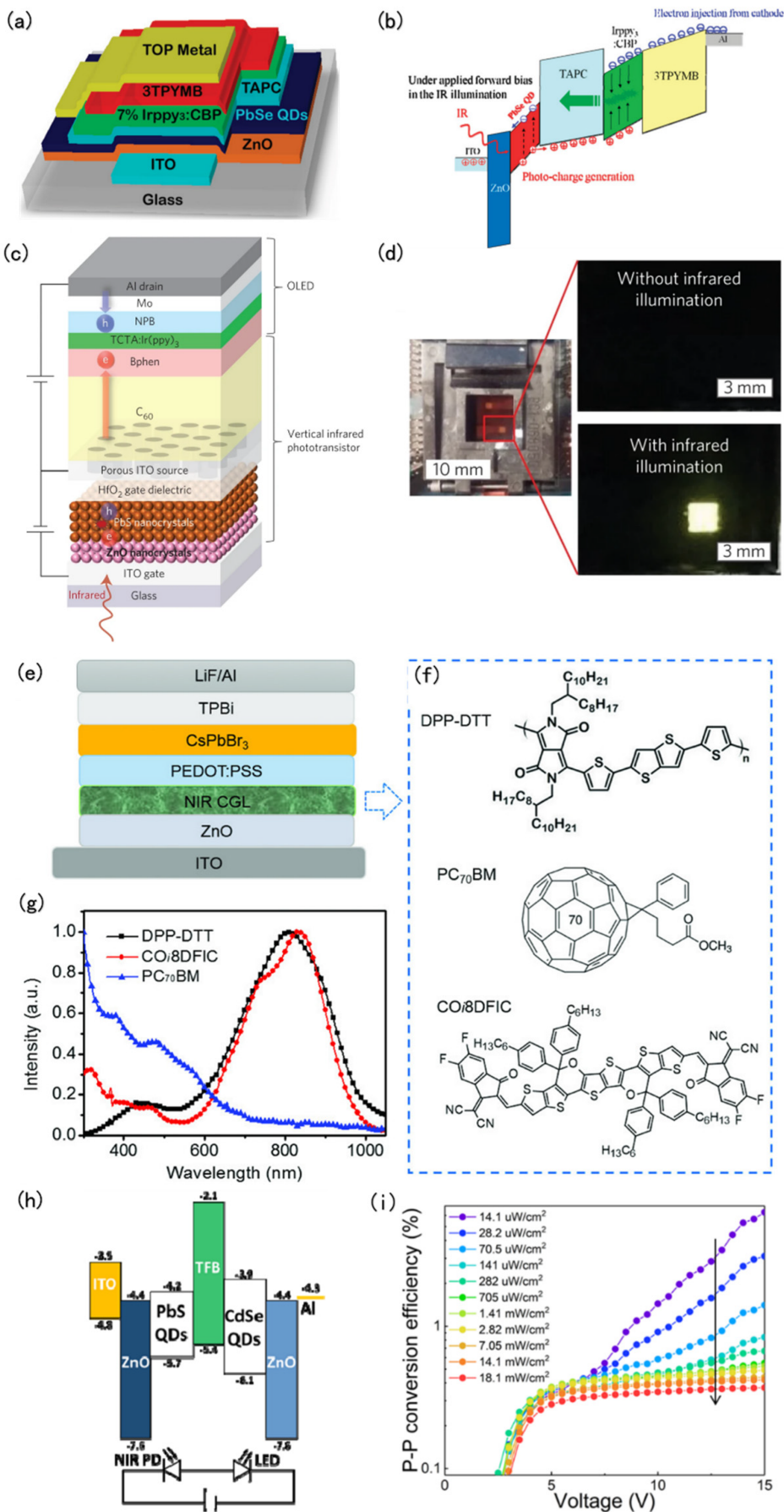


**Figure 1.** Structures and performance characterization of QDs based NIR-to-visible upconversion devices. **(a)** Structure of PbSe QD infrared-to-green light upconversion device. **(b)** Schematic energy band diagrams of PbSe QD upconversion devices in the IR illumination [1]. Copyright 2011, Nano Letters. **(c)** Structure of the upconversion device. As shown in the diagram, the colloidal nanocrystals PbS are used as a gate sensitized to the infrared, and an ITO porous layer is used as source electrode of the phototransistor. **(d)** Photo of the sample attached to the measuring case in ambient light (left), and photos of the area of the device (0.04 cm<sup>2</sup>) with and without infrared lighting ( $\lambda = 940$  nm), absent ambient light (right) [2]. Copyright 2016, Nature Photonics. **(e)** Diagram showing the cross-section view of a NIR–visible light upconversion device, with a NIR photodiode and a visible light LED based on CsPbBr<sub>3</sub> perovskite. **(f)** Molecular structures of DPP–DTT, PC<sub>70</sub>BM, and CO<sub>8</sub>DFIC, and **(g)** their corresponding normalized absorbance spectra [3]. Copyright 2018, Advanced Optical Materials. **(h)** The structure of the conversion system and circuit show, schematically, the principle of operation of this upconversion device. **(i)** The photon-to-photon conversion efficiency of the device, under different power densities of NIR, as a function of the applied voltage [4]. Copyright 2020, IEEE Access.

In 2016, Yu et al. reported a novel upconversion light-emitting phototransistor (LEPT) by incorporating a phosphorescent OLED into a phototransistor. To be different from the ascending upconverters with two terminals, this LEPT is a vertical three-terminal phototransistor with an infrared photoactive gate integrated into an OLED, which has high-efficiency such as its external quantum efficiency (EQE) of up to  $1 \times 10^5\%$  and detectivity of  $1.23 \times 10^{13}$  Jones [2]. The structure of this LEPT is demonstrated in **Figure 1c**, and a photograph of the sample clamped in the measurement box is shown in **Figure 1d**. In 2018, Li et al. demonstrated a perovskite LED based on CsPbBr<sub>3</sub> with high performance, it can be processed in solution and has a narrow emission spectrum. Their research proved that the NIR-sensitive polymer DPP–DTT blend with a norfullerene acceptor CO<sub>8</sub>DFIC is an appropriate layer of charge generation layer for the upconversion procession, as a result of its unique combination of high NIR absorption and low visible light absorption (**Figure 1e–g**) [3]. In 2020, Tang and his co-workers proposed a high conversion efficiency for all QDs-based upconverters (**Figure 1h**). Former upconversion systems were always manufactured by inorganic semiconductors using wafer fusion technology. However, they were limited by the mismatch of lattice between different semiconductors, leading to poor photonic conversion efficiency. As for the all-organic devices, their efficiency has been improved a lot, but the stability of these upconverters is still a potential issue for their application. In this reference, the use of innately stable, efficient, and high-performance QDs made the device achieve a high photon-to-photon conversion efficiency of 6.3% (**Figure 1i**), and can be fabricated by solution process [4].

## 2. SWIR-to-Visible Upconversion

In 2020, Ning Zhijun's research group from ShanghaiTech University integrated CQD infrared detectors and colloidal QLED for the first time to obtain a CQD infrared-to-visible light upconversion device (**Figure 2a**). This all-CQDs upconversion device had high photonic conversion efficiency of up to 6.5%, and it can be turned on at a low applied bias of only 2.5 V. Through this upconverter the short-wave infrared (**Figure 2b**) with a power density of 10–600 mW·cm<sup>-2</sup> was converted into visible green light (520 nm) (**Figure 2c**). Ning's group incorporated silver

nanoparticles in the PD's layers that can extract charges (**Figure 2d**) with the aim of optimizing the carrier tunneling and making the PD layer provide enough photocurrent so that the LED can be turned on successfully. This advanced achievement confirms the application of CQDs in upconversion devices and the feasibility of realizing SWIR upconversion imaging [5].

**Figure 2.** Structures and performance characterization of CQDs based SWIR-to-visible upconversion devices. **(a)** Structure and composition of upconversion devices. **(b)** Photoluminescence spectra of CdSe/ZnS core/shell QDs, with the peak position at 525 nm. Inset: transmission electron microscopy (TEM) of CdSe/ZnS QDs. **(c)** Absorbance of PbS QD thin films, with the exciton peak position at 1500 nm. Inset: TEM of PbS QDs. **(d)** PD energy band graph with Ag nanoparticles in ZnO film. Without Ag nanoparticles (top) or in darkness (middle), the hole transfer from the ITO film to ZnO is blocked by the energy level shift. Under the lighting (bottom), holes enter the ZnO film [5]. Copyright 2020, Nature Electronics.

### 3. MIR-to-Visible Upconversion

In 2020, Motmaen reported a novel and high-performance integrated chip which can realize the upconversion process from MIR (3–5  $\mu\text{m}$ ) to the green light (523 nm). This upconversion device was fabricated using a doped PbSe layer as a PD, an NPN (*n*-type, *p*-type, *n*-type) bipolar junction transistor (NPN-BJT) as a current amplifier, and an OLED as an emission layer; its structure is shown in **Figure 3a**, the energy band diagram is shown in **Figure 3b**. In this new type of upconverter, PbSe QDs were used to realize the photodetection and generate current, then the output electric information can be amplified by NPN-BJT. With the amplified current the LED can be driven and emits visible green light [6]. Under 3  $\mu\text{m}$  MIR light illumination (0.5  $\text{mW}/\text{cm}^2$ ) (**Figure 3c**) and total voltage of 13.5 V, the EQE is calculated to 600% (**Figure 3d**), such high EQE is mainly thanks to the amplifier function of NPN-BJT.

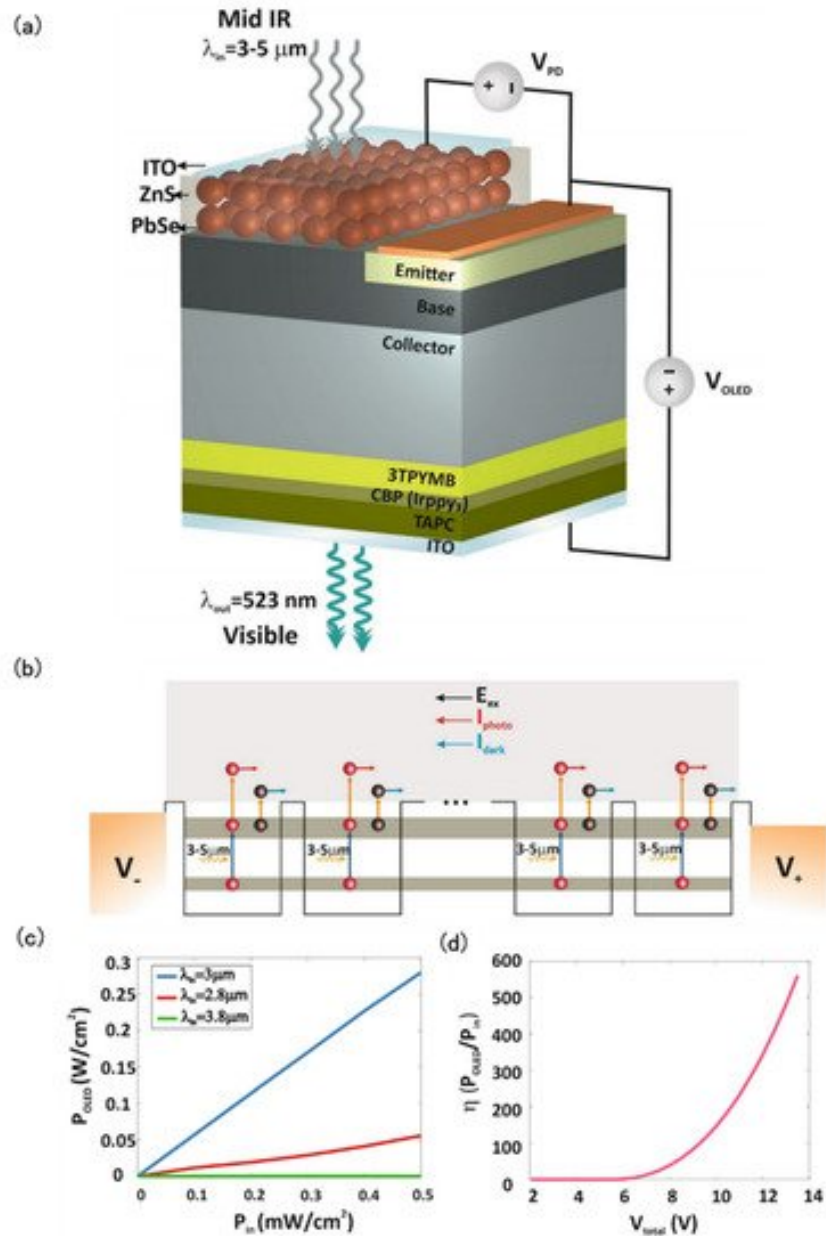


**Figure 3.** Structures and performance characterization of CQDs-based MIR-to-visible upconversion devices. (a) Structure of MIR-to-visible light upconversion device. (b) Schematic shows the energy band diagram of the PbSe/ZnS quantum dots PD and the transition inside PD. The transfer of electrons from the energy levels of the excited state to the continuum by means of the thermal energy of the environment causes a dark current (black circle,  $I_{\text{dark}}$ ). The photons excite electrons from energy levels of ground state to energy levels of excited state, resulting in a photocurrent (red circle,  $I_{\text{photo}}$ ). (c) The output power density depending on the lighting power density MIR with different wavelengths. (d) The efficiency of PbSe upconversion device as function of the applied voltage under MIR light illumination ( $\lambda = 3 \mu\text{m}$ ,  $0.5 \text{ mW/cm}^2$ ) [6]. Copyright 2020, Scientific Reports.

The liquid semiconductor QDs synthesized by colloidal chemistry can precisely tune the bandgap by adjusting the size, and then achieve tunable infrared photoresponse in a wide spectral range. Therefore, from the above

demonstration, it can be seen that the application of CQDs in the field of infrared-to-visible upconversion can realize infrared detection in all main infrared bands of NIR, SWIR, and MIR.

After several decades of development, infrared-to-visible upconversion devices have shown a transition trend from traditional all-inorganic, all-organic, and organic-inorganic materials to emerging liquid CQD materials. The development of infrared-to-visible light upconversion devices based on CQDs has become one of the important trends to achieve wide detecting spectrum, high-performance, low-cost, flexible, and large-area infrared imaging in the future. The performance of the upconversion devices in the references discussed above is shown in **Table 1**.

**Table 1.** Progress in upconversion devices.

Year	Detect Material	Emit Material	Type	Detect Range (nm)	Emission	Maximum Conversion Brightness ( $\text{cd/m}^2$ )	Efficiency (%)	Ref.
2011	PbSe	CBP: $\text{Ir(ppy)}_3$	CQD	1500 (peak:1300)	Green (550 nm)	5	1.3	[1]
2016	PbS	TATC: $\text{Ir(ppy)}_3$	CQD	940~1042	Green (550 nm)	~100	1597	[2]
2018	DPP- DTT: $\text{COi8DFIC}$	$\text{CsPbBr}_3$	CQD	850	Green (520 nm)	~300	1.7	[3]
2020	PbS	CdSe	CQD	970	Red (624 nm)	155	6.3	[4]
2020	PbS	CdSe/ZnS	CQD	400~1600	Green (525 nm)	~600	6.5	[5]

Year	Detect Material	Emit Material	Type	Detect Range (nm)	Emission	Maximum Conversion Brightness (cd/m <sup>2</sup> )	Efficiency (%)	Ref.
2020	PbSe	CBP: Ir(ppy) <sub>3</sub>	CQD	3000–5000	Green (523 nm)	-	-	

CBP: 4,4-N, N-dicarbazole-biphenyl; Ir(ppy)<sub>3</sub>: fac-tris(2-phenylpyridinato) iridium (III).

## References

1. Kim, D.Y.; Choudhury, K.R.; Lee, J.W.; Song, D.W.; Sarasqueta, G.; So, F. PbSe Nanocrystal-Based Infrared-to-Visible Up Conversion Device. *Nano Lett.* 2011, 11, 2109–2113.
2. Yu, H.; Kim, D.; Lee, J.; Baek, S.; Lee, J.; Singh, R.; So, F. High-gain infrared-to-visible upconversion light-emitting phototransistors. *Nat. Photonics* 2016, 10, 129–134.
3. Li, N.; Lau, Y.S.; Xiao, Z.; Ding, L.; Zhu, F. NIR to Visible Light Upconversion Devices Comprising an NIR Charge Generation Layer and a Perovskite Emitter. *Adv. Opt. Mater.* 2018, 6, 1801084.
4. Tang, H.; Shi, K.; Zhang, N.; Wen, Z.; Xiao, X.; Xu, B.; Butt, H.; Pikramenou, Z.; Wang, K.; Sun, X.W. Up-conversion device based on quantum dots with high-conversion efficiency over 6%. *IEEE Access* 2020, 8, 71041–71049.
5. Zhou, W.; Shang, Y.; García de Arquer, F.P.; Xu, K.; Wang, R.; Luo, S.; Xiao, X.; Zhou, X.; Huang, R.; Sargent, E.H.; et al. Solution-processed upconversion photodetectors based on quantum dots. *Nat. Electron.* 2020, 3, 251–258.
6. Motmaen, A.; Rostami, A.; Matloub, S. Ultra High-efficiency Integrated Mid Infrared to Visible Up-conversion System. *Sci. Rep.* 2020, 10, 9325.

Retrieved from <https://encyclopedia.pub/entry/history/show/50777>